Research Article

Hui Yang* and Wenhui Chen

Study on the reliability of nano-silver-coated tin solder joints for flip chips

https://doi.org/10.1515/gps-2023-0137
received July 29, 2023; accepted October 9, 2023

Abstract: The nano-silver-coated tin (Sn@Ag) paste was modeled using the method of the Anand unified viscoplastic constitutive model and elastic model. After thermal cyclic loading, the plastic strain of the solder joints increased cumulatively, while the maximum equivalent stress remained basically stable. The simulation results show that the maximum displacement occurs at the solder joint at the farthest end from the center of the chip, which is a dangerous solder joint. Using the finite element method and EPRI (the American Electric Power Research Institute) estimation method, the fatigue life of the nano-silver-coated tin solder joint is predicted to be 616 weeks, which is significantly higher than that of the nano-silver solder joint. It is indicated that adding a certain amount of nano-tin to the nano-silver paste to form a core–shell structure can improve the shear strength of the solder joint and reduce the plastic strain, thereby significantly improving the reliability of the solder joint. It is proved by experiments that the nano-silver paste is feasible for flip–chip interconnection. The research on this topic provides experimental reference and theoretical basis for the application of a new generation of interconnection materials in power devices and promotes the development and application of microelectronic packaging technology.

Keywords: flip chip, nano-silver-coated tin, fatigue life

1 Introduction

Nanoscale silver paste is widely used in chip connection but its application is limited by high sintering temperatures and low bonding strengths. The addition of low melting point alloying elements is a good way to reduce the sintering temperature and increase the sintering strength of the nano-silver slurry [1]. Among doped metals, tin, indium, and gallium all have low melting points but the cost of indium and gallium is relatively high; therefore, we choose nano tin as a dopant [2]. Considering that tin is easy to be oxidized, and the core–shell material can prevent tin oxidation and ensure the uniform distribution of tin in the matrix, this study adopts the scheme of preparing the core–shell material Sn@Ag.

The sn-silver solid solution and the intermetallic compound Ag_3Sn (strengthened phase) were formed by sintering the nano-Sn@Ag slurry. When the content of tin is 5%, the sintering strength of the nanometer Sn@Ag slurry is the highest [3], and the ratio of Ag_3Sn particles to Ag matrix is 1:5 after sintering. The hardness of the intermetallic compound Ag_3Sn is very high, so the plastic strain generated by the solder joint is mainly formed by the silver matrix. Therefore, in this article, Ag_3Sn is regarded as an elastic material in finite element modeling and expressed by the elastic equation [4]. The matrix Ag is regarded as a viscoplastic material and is expressed by the Anand constitutive equation [5]. This study considers inverted solder joints as an example. The diameter of nano-silver-coated tin solder joints is 100 μm, and the bottom plate is a PCB board, as shown in Figure 1.

2 Finite element analysis of the nano Sn@Ag solder joint

2.1 Anand constitutive equation and parameter determination

The relation between the saturation stress and strain rate of the viscoplastic Anand model is as follows:

$$\sigma^* = \frac{s'}{\xi}\left[\frac{\dot{\varepsilon}_p}{A}\exp\left(\frac{Q}{RT}\right)\right]^n \sinh^{-1}\left\{\left[\frac{\dot{\varepsilon}_p}{A}\exp\left(\frac{Q}{RT}\right)\right]^m\right\} \quad (1)$$

The relationship between stress and strain at different temperatures and different strain rates can be expressed as follows:

* **Corresponding author: Hui Yang**, College of Mechanical and Control Engineering, Guilin University of Technology, 541004, Guangxi, China, e-mail: 474055963@qq.com
Wenhui Chen: College of Mechanical and Control Engineering, Guilin University of Technology, 541004, Guangxi, China

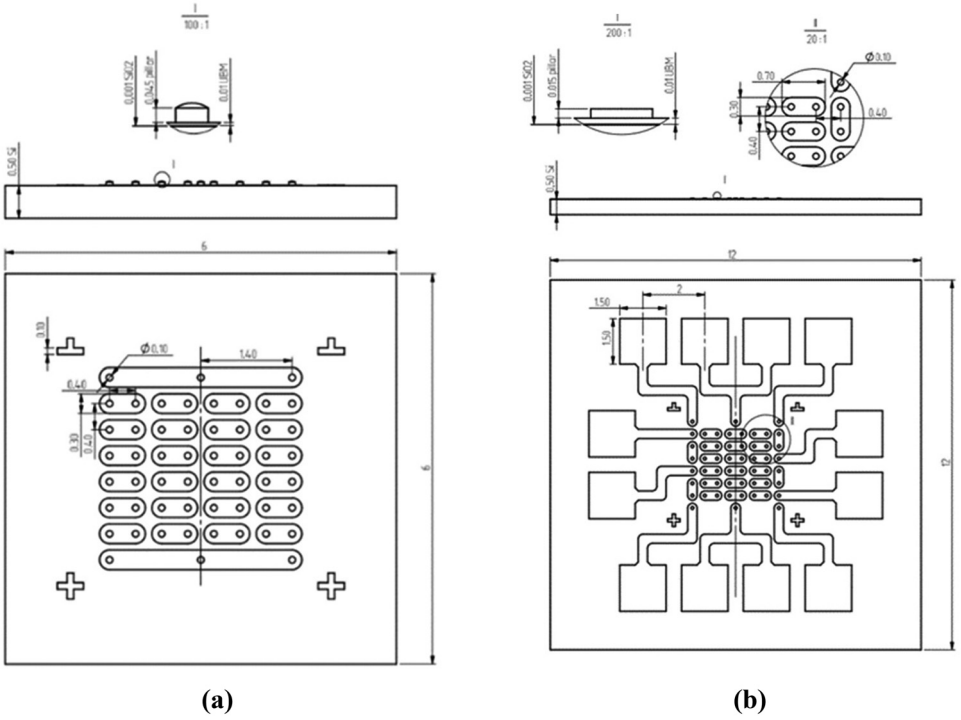

Figure 1: Flip chip and the bottom plate: (a) flip chip (silicon) and (b) baseboard (PCB).

$$\sigma = \sigma - \{(\sigma - cs_0)^{(1-\alpha)} + (\alpha - 1)[(ch_0)(\sigma)^{-\alpha}]\varepsilon_p\}^{\frac{1}{(1-\alpha)}}, \quad \alpha \neq 1 \tag{2}$$

The above equation contains the nine parameters of the Anand constitutive equation:

A, Q/R, ξ, s', n, m, α, h_0, and s_0, and are defined respectively as a constant, the activation energy/gas constant, stress multiplier, the saturation value coefficient of deformation impedance, the strain rate sensitivity, the strain rate sensitivity index, the strain hardening parameter, the strengthening coefficient, and the initial value of deformation impedance. The constitutive equation model parameters of the nanosilver matrix are listed in Table 1 [6].

2.2 Finite element model of the solder joint

This chip module model is composed of three parts: the upper part is made of a Si chip, the lower part is made of a printed circuit board (PCB), and the middle part is made of a Cu column and nano Sn@Ag solder joint. For the convenience of operation, it is assumed that a solder joint contains a cylindrical Ag_3Sn with a thickness of 0.004 mm, which is distributed in the middle of the Ag matrix, as shown in Figure 2a. Ag_3Sn particles are replaced by this structure. In the finite element analysis software Work-Bench, because of symmetry, the 1/4 structure is selected to build a model and analyze it. The model of 3D and 2D model modeling can also be used at this time, but the 3D mesh model is more complex, as the system calculation takes longer; however, model using 2D modeling can simplify the mesh, reduce the calculation time, and achieve similar results, as shown in Figure 2b.

The material properties of each component are shown in Table 2 [7]. The elastic modulus, Poisson's ratio, and thermal expansion coefficient of the Si chip, PCB board, Cu column, Ag_3Sn, and nano-Ag are listed in Table 2.

2.3 Stress–strain analysis of solder joints

The thermal cycling load is determined according to various conditions that may be encountered during service.

Table 1: Anand model parameters of the nano-silver matrix

A (s^{-1})	Q/R (1/k)	m	n	ξ	s' (MPa)	h_0 (MPa)	s_0 (MPa)	α
9.81	5,709	0.6572	0.00326	11	67.389	15,800	2.768	1

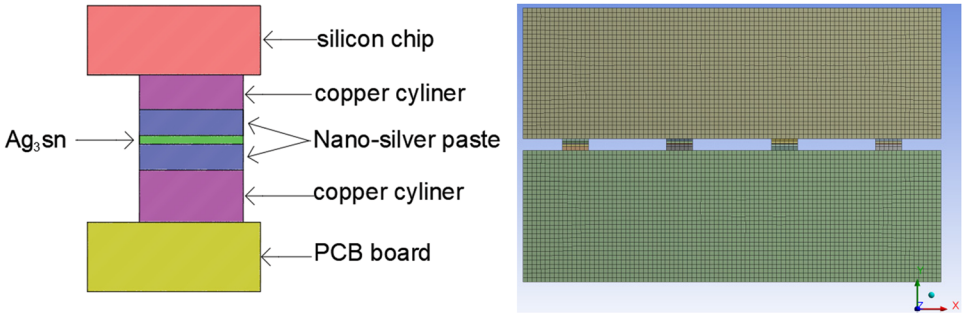

Figure 2: (a) Finite element modeling and (b) meshing.

Table 2: Material properties of chip components

Component	Modulus of elasticity (GPa)	Poisson's ratio	Coefficient of thermal expansion (10^{-6} per °C)
Chip(Si)	131	0.3	2.8
Copper pillar	110	0.34	16.4
Ag_3Sn	80	0.35	18
Nano-silver	6.28	0.37(25°C)	19.6
FR-4	17.2	0.28	16

The temperature range is −50°C to 150°C and the temperature rise and fall rate are 25°C·min^{-1}; The cycling load is maintained for 10 min when it rises to the highest temperature and 10 min when it is lowered to the lowest temperature. The cycle period is 36 min, and this model calculates 5 cycles.

When the chip is subjected to a thermal load, it first produces a certain degree of displacement, that is, deformation. Figure 3 shows the displacement diagram of chip components and single solder joint under multiple cycle temperature loads. As shown in Figure 3a, the solder joint farthest from the chip center has the largest displacement and is a dangerous solder joint. This is mainly because the central part of the chip is fixed and constrained, while the other parts of the chip are free. According to the principle of thermodynamics, the farther the solder joint is from the center of the chip, the larger its deformation will be. As shown in Figure 3b, under multiple periodic temperature loads, the contact area between the dangerous solder joint and the copper column shows obvious displacement, while the displacement in the internal area of the solder joint is small. This is mainly because the thermal expansion coefficient of the nano-silver–tin solder and copper column is different from each other, and as the deformation degree of the two is different, there is obvious displacement at the contact interface of the two. As the solder joint internal material is the same and the deformation difference is not big, the solder joint internal displacement is small.

Figure 4 shows the stress diagram of the hazardous solder joint. It can be seen that the area where the solder joint is connected to the Cu column generates significant stress, while the stress distributed inside the solder joint is small. Figure 5 is the stress curve of the dangerous solder joint, from which it can be seen that the maximum equivalent stress basically remains unchanged with the increase of the number of periodic temperature loads. However, it can be observed from the stress–strain curve of the solder joint in Figure 6 that the plastic strain of the solder joint has a cumulative process over time. This is mainly because when the thermal load reaches 150°C, the deformation of the solder joint has exceeded the elastic range, and the plastic strain begins to occur. The plastic strain is an unrecoverable deformation so although the maximum stress remains basically unchanged, the plastic strain will gradually increase through a cumulative process. It can be predicted that the plastic strain of the dangerous solder joint will gradually increase with the continuous loading of the periodic temperature load, which will eventually cause chip failure.

In order to analyze the plastic deformation of inverted solder joints under periodic temperature loading in more detail, the plastic strain loading history of dangerous solder joints was studied. Figure 7 shows the relation curve between the plastic strain and time of dangerous solder joints of the nano-silver-coated tin solder.

3 Reliability analysis of the nano-Sn@Ag solder joint

Under the action of a periodic temperature load, the distribution of stress and strain of the solder joint is variable,

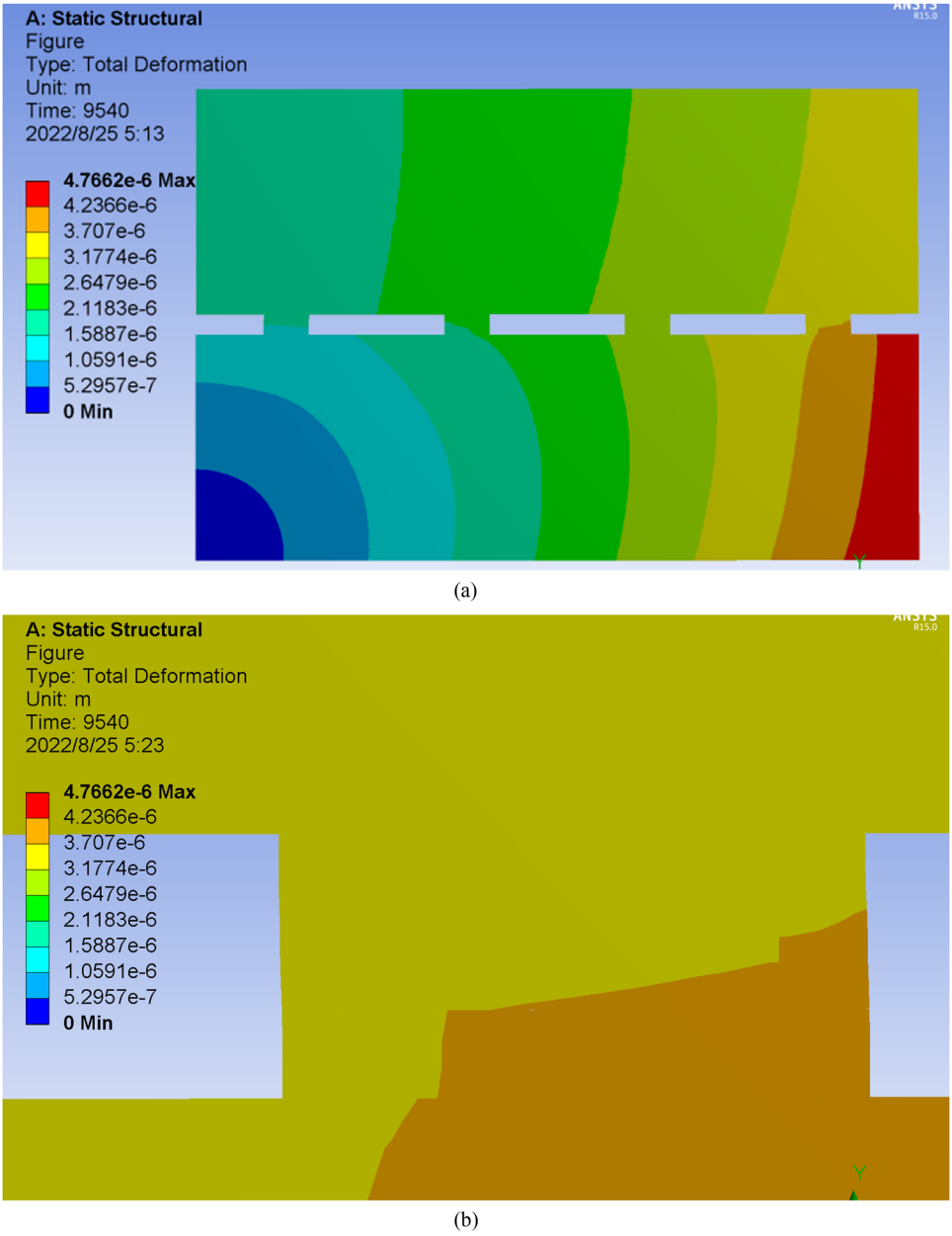

Figure 3: Solder joint displacement diagram of the flip chip: (a) interconnect chip and (b) dangerous solder joints.

and not only time and pressure parameters can affect the reliability of welding, but also the sintering temperature and solder composition and other factors affect the performance of the solder joint. According to experience, plastic strain can cause cracking of solder joints and lead to failure of solder joints, and the Coffin–Manson (C-M)-modified model is a fatigue equation related to plastic strain. Therefore, this project adopts this model in the finite element to predict the life of nano-Sn@Ag solder joints.

Since the 1960s, according to the COD theory and J-integral elastic–plastic fracture mechanics theory, some teams have derived the failure criterion of crack development under large yield deformation, that is, $\delta \le \delta_c$, $J \le J_{IC}$, so that the fatigue life of the crack can be calculated by calculating the J-integral. Meanwhile, in engineering practice, this article uses the American Electric Power Research Institute (EPRI) engineering method to estimate the J integral and calculate the solder joint life. This method can predict fatigue life without using the finite element

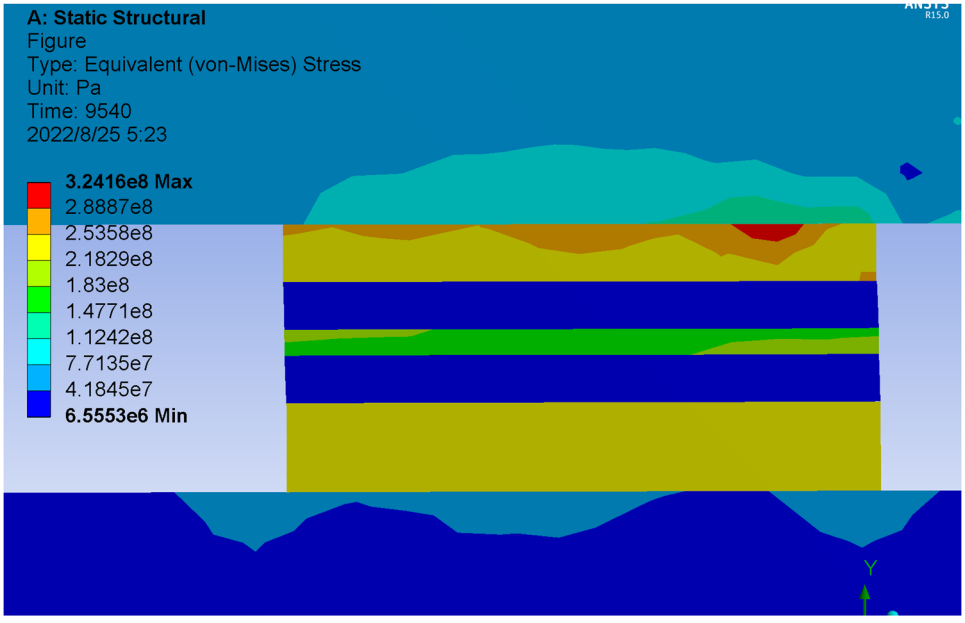

Figure 4: Equal stress diagram of the dangerous solder joint.

method, which is an estimation method other than the finite element method.

3.1 Prediction of the fatigue life of solder joints by the finite element method

The modified equation of C–M proposed by Engel–Maier has become a more reasonable one among the many derivative equations, and the calculation conclusion with this equation will be more accurate, which is widely used in the derivation of fatigue cycle number of solder joints and other fields:

$$N_f = \frac{1}{2}\left(\frac{\Delta\gamma}{2\varepsilon_f'}\right)^{\frac{1}{c}} \tag{3}$$

By using finite element software to calculate the strain range of the inner nodes of the nano-silver–tin slurry, the solder joints in the most dangerous areas can be found. $\Delta\varepsilon = 0.01472$ of

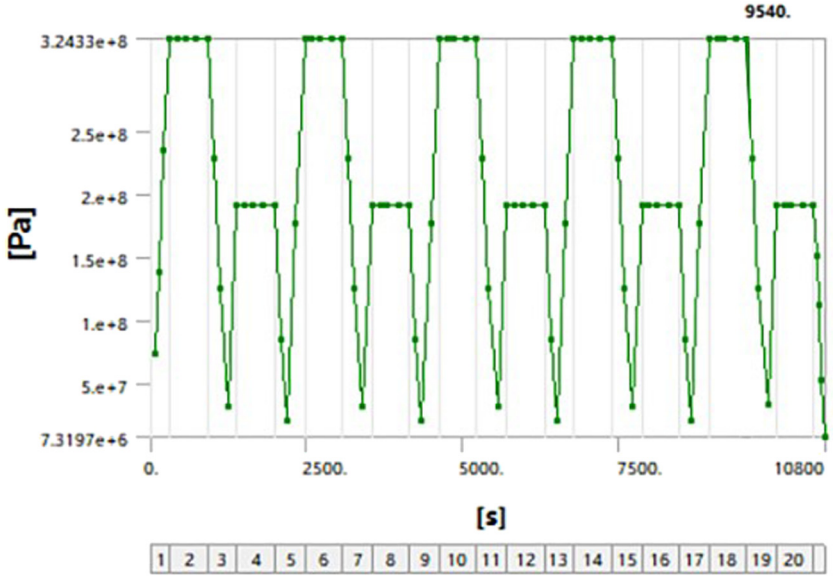

Figure 5: Relation between the equivalent stress of the dangerous solder joint and time.

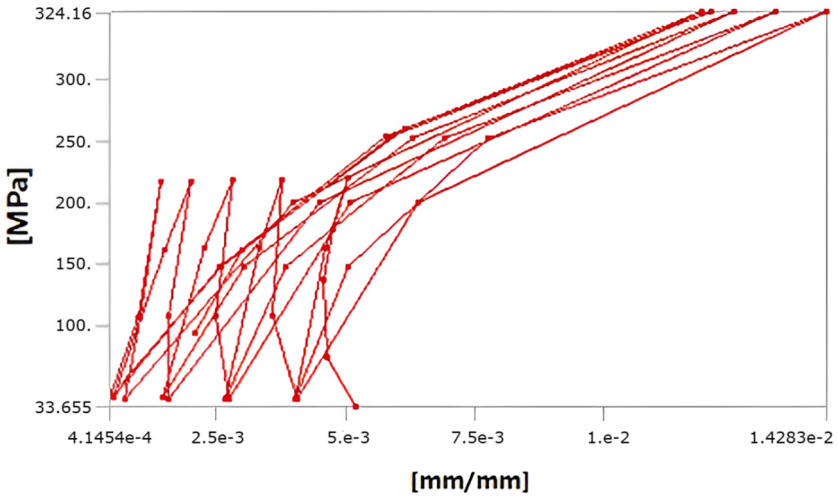

Figure 6: Stress–strain curve of the solder joint.

the solder joint and the derived $\Delta\gamma = 0.0255$. The T_m of the periodic temperature load is equal to 50°C, and each thermal cycle is 36 min. It can be deduced that $f = 1.67$ cycles per h and $C = -0.455$ when substituted into the formula. The fatigue life of the solder joints of the nano-silver–tin slurry can be calculated by inserting the above data into Eq. 3.

The fatigue cycles of pure nano-silver solder joints and nano-Sn@Ag solder joints were calculated by the derivation study, and are listed in Table 3. The results show that the cycle failure times of the nano-Sn@Ag solder joint are significantly higher than that of the pure nano-Ag solder joint. According to the previous experiment, it can be predicted that after doping with alloying element Sn, the nano-Ag_3Sn phase is formed during the sintering process of the nano-Ag-Sn slurry, which plays the role of second phase strengthening.

Table 3: Comparison of fatigue cycles of two solder joints

Solder joints	$\Delta\varepsilon$	$\Delta\gamma$	N_f
Nano-silver	0.0173	0.02966	432
Nano-silver + Ag_3Sn	0.01472	0.0255	616

3.2 Prediction of the fatigue life of solder joints by the EPRI engineering estimation method

The J-integral engineering estimation method was introduced by the EPRI for the first time [8,9]. This method has the advantages of fewer parameters, a simple calculation process, etc., and has been widely used in fatigue life

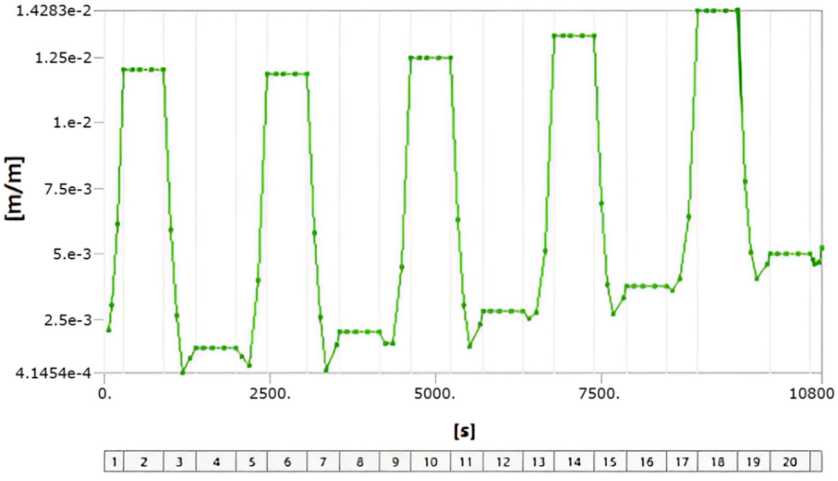

Figure 7: Equivalent plastic strain curve of the dangerous solder joint.

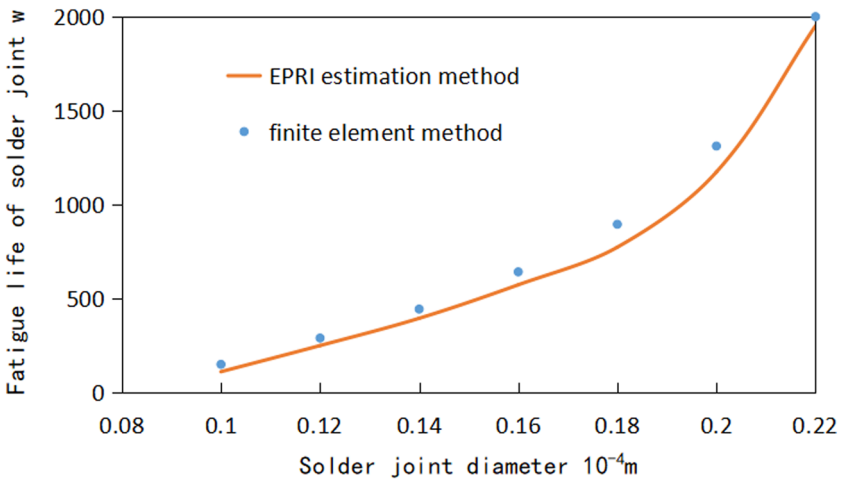

Figure 8: Influence of the solder joint diameter on fatigue life calculated using the two methods.

estimation [10,11]. The estimation method is to decompose the J-integral into linear and nonlinear components [12,13].

From the initial crack size to the critical size integral, we have [14]

$$\int_{a_o}^{a_c} \mathrm{d}a = xJ^r \int_0^{N_f} \mathrm{d}N \tag{4}$$

where a is the crack size, x and r are material constants, J is the J-integration, and N_f is the fatigue life. The fatigue life N_f can be calculated from Eq. 4. The theoretical results are in agreement with the fatigue life predicted by the finite element method, which is 616 weeks.

3.3 Calculation of the influence of solder joint topography on fatigue life using two different methods

The EPRI estimation method and the finite element method were used to calculate the influence of the solder joint diameter change on the fatigue life. The single-factor experiment method was used to select seven different diameters as research targets while keeping the solder joint height unchanged. The diameters selected successively were 0.10, 0.12, 0.14, 0.16, 0.18, 0.20, and 0.22 (unit: $\times 10^{-4}$ m).

As shown in Figure 8, the horizontal coordinate refers to the diameter of the solder joint, and the vertical coordinate refers to the number of fatigue cycles of the solder joint. According to the figure, as the diameter of the solder joint continues to increase, the plastic strain range of the internal joints decreases, and the derived thermal fatigue life gradually increases. From the comparison of the calculation results of the two methods, it can be seen that they are in good agreement, which proves that the C–M modified model has higher calculation accuracy.

The EPRI estimation method and the finite element method were used to calculate the influence of the solder joint height variation on fatigue life, and the single-factor experiment method was used to select seven different heights as research targets under the condition that the

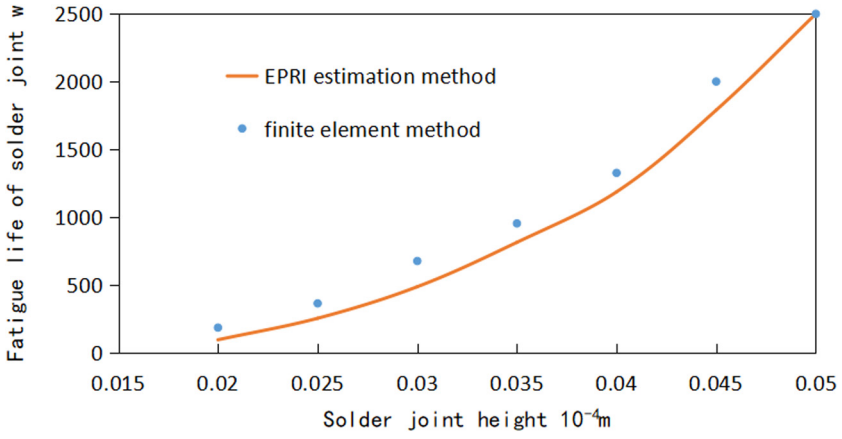

Figure 9: Influence of the solder joint height variation on fatigue life calculated using the two methods.

solder joint diameter remained unchanged. The height values selected in turn were 0.02, 0.025, 0.03, 0.035, 0.04, 0.045, and 0.05 (unit: $\times 10^{-4}$ m).

As shown in Figure 9, the horizontal coordinate refers to the height of the solder joint, and the vertical coordinate refers to the fatigue life of the solder joint. According to the figure, as the height of the solder joint increases, the plastic strain range of the joint decreases, and the derived thermal fatigue life increases gradually. According to the slope degree of the curve, the change in height has a stronger correlation with the thermal fatigue life of the solder joint. A comparison between the EPRI estimation method and finite element method shows that they are in good agreement, which proves that FEM has high calculation accuracy and wide application range.

4 Summary

The nano-Sn@Ag solder was modeled using the Anand constitutive model and the elastic model, and the simulation results provide a certain reference for the finite element analysis of the particle-enhanced nano-solder to promote the development of research on the interconnect reliability of the nano-silver slurry.

1) Using finite element simulation, it was determined that the maximum displacement of chip components occurs at the junction of the solder joint and copper column, which is a dangerous area. Although the equivalent stress of the solder joint remains stable after thermal cycling, its plastic strain will accumulate and increase, which will lead to the ultimate failure of the interconnect chip.
2) After five cycles of thermal cycle load, the equivalent plastic strain range of the chip dangerous solder joint was found to be 0.01472, and the plastic shear strain range of the solder joint was 0.0255. Using the C–M correction equation, the thermal fatigue cycle number of the nano-silver-coated tin solder joint was derived to be 616 weeks.
3) The finite element method and the EPRI estimation method were used to calculate the results, and it was found that the fatigue cycle number of nano-Sn@Ag solder joints was significantly higher than that of nano-Ag solder joints, indicating that the addition of a certain amount of Sn element to the nano-silver paste could improve the shear strength of solder joints and thus increase the number of thermal fatigue cycles of solder joints.

Funding information: The authors state that no funding was involved.

Author contributions: Hui Yang: writing – review & editing, methodology, and formal analysis. Wenhui Chen: writing – original draft, visualization, and project administration.

Conflict of interest: The authors state no conflict of interest.

Data availability statement: The datasets generated during and/or analyzed during the current study are available from the corresponding author on reasonable request.

References

[1] Tsai CH, Huang WC, Chew LM, Schmitt W, Li J, Nishikawa H, et al. Low-pressure micro-silver sintering with the addition of indium for high-temperature power chips attachment. J Mater Res Technol-JMR&T. 2021;15:4541–53.
[2] Qiwang C. Preparation and Properties of Nano-tin modified nano-silver paste for Power chip Interconnect. Master's Thesis. South China University of Technology; 2018.
[3] Yang CX, Li X, Lu GQ, Mei YH. Enhanced pressureless bonding by Tin Doped Silver Paste at low sintering temperature. Mater Sci Eng A. 2016;660:71–6.
[4] Lu XZ, Lv Z, Sun Q, Murugesan M, Zhou C, Zhang X, et al. Enhanced mechanical and thermal properties of Ag Joints Sintered by Spark Plasma Sintering. J Electron Mater. 2022;51(11):6310–9.
[5] Su YT, Fu GC, Liu CQ, Zhang K, Zhao L, Liu C, et al. Thermo-elasto-plastic phase-field modelling of mechanical behaviours of sintered nano-silver with randomly distributed micro-pores. Comput Methods Appl Mech Eng. 2021;378:113729.
[6] Yu DJ, Chen X, Chen G, Lu GQ, Wang ZQ. Applying Anand model to low-temperature sintered nanoscale silver paste chip attachment. Mater Des. 2009;30(10):4574–9.
[7] Guo SJ. Meso-cyclic constitutive model for ratcheting behavior of particle-reinforced metal matrix composites. Doctoral Dissertation. Southwest Jiaotong University; 2012.
[8] Kumar V, German MD, Wilkening WW. Translated by Institute of Engineering Mechanics, Tsinghua University. The progress of EPRI NP-3607 plastic fracture analysis. Beijing: Tsinghua University Press; 1984. p. 48–64.
[9] Zikry M. Ductile fracture. Handb Mater Modeling. 2005;(25):1171–81.
[10] Sun L, Li PN, Liu CJ. Equivalent remote stress method of J-integral evaluation for any stress-strain relationship materials. J Mech Strength. 2003;25(4):450–5.
[11] Zahoor A. Evaluation of J-integral estimation scheme for flawed through-wall pipes. Nucl Eng Des. 1987;100(1):1–9.
[12] Guoqiang D. Fracture parameters of miter bend inner crack. Master Dissertation. Dalian University of Technology; 2009.
[13] Qi X, Lv YB, Xu ZX. The determining of Ramberg-Osgood-shaped power hardening material's hardening factor and hardening exponent. J Wuhan Transp Univ. 1996;20(3):319–22.
[14] Sun P, Andersson C, Wei XC, Cheng ZN, Shangguan DK, Liu J Coffin-Manson constant determination for a Sn-8Zn-3Bi lead-free solder joint Solder. Surf Mt Technol. 2006;18(2):4–11.